LASER INTERFEROMETER GRAVITATIONAL WAVE OBSERVATORY

LIGO Laboratory / LIGO Scientific Collaboration

LIGO-T070021-00-D *ADVANCED LIGO* Date: 08-20-07

Status of High Power Measurements in Faraday Isolators

Rodica M. Martin for the IO Group, University of Florida

Distribution of this document:
LIGO Science Collaboration

This is an internal working note
of the LIGO Project.

California Institute of Technology
LIGO Project – MS 18-34
1200 E. California Blvd.
Pasadena, CA 91125
Phone (626) 395-2129
Fax (626) 304-9834
E-mail: info@ligo.caltech.edu

Massachusetts Institute of Technology
LIGO Project – NW17-161
175 Albany St
Cambridge, MA 02139
Phone (617) 253-4824
Fax (617) 253-7014
E-mail: info@ligo.mit.edu

LIGO Hanford Observatory
P.O. Box 1970
Mail Stop S9-02
Richland WA 99352
Phone 509-372-8106
Fax 509-372-8137

LIGO Livingston Observatory
P.O. Box 940
Livingston, LA 70754
Phone 225-686-3100
Fax 225-686-7189

http://www.ligo.caltech.edu/

1 Introduction

As part of Advanced LIGO, optical powers as high as 180 W will be required. Consequently, optical absorption in the Faraday Isolators, as well as aspects like thermal lensing, thermal drift, and thermal birefringence will need to be reconsidered. This document is an update on Advanced LIGO Faraday Isolator design, in particular, investigations of the optical isolation, thermal drift and thermal lens compensation.

2 Summary of Measurements

The Faraday Isolator (FI) is responsible for rejecting the back-reflected light from propagating towards the MC, which otherwise would induce phase noise in the interferometer. At high optical powers, absorption in the FI optical components generates thermally induced birefringence, thermal lensing and beam steering, therefore requiring alternative designs and compensation methods, as well as a careful selection of the polarizers and crystals[1].

A new FI design proposed for Advanced LIGO is based on a set of three polarizers: a pair of calcite wedge polarizers (CWP) and a thin film polarizer (TFP) inserted in between. This design is intended to optimize both the isolation and the beam steering of the back-reflected beam. To attain a better feeling about the provenience and the magnitude of the different performances, we conducted high power tests on Faraday Isolators in two separate configurations:

- first, using our self-compensating Faraday Rotator (FR) with a combination of a fused-silica thin film polarizer and a calcite wedge polarizer (TFP + CWP);
- second, using two identical calcite wedges (CWP + CWP).

In each configuration we investigated:

- optical isolation
- thermal drift
- compensation for thermal lensing[2]

The measurements were made in air, using a beam diameter of 3.9 mm, within 10 % the value intended for use in Advanced LIGO.

We found isolation as high as **39 dB** for the **TFP + CWP** geometry and **49 dB** for the **CWP + CWP** setup at **103 W** input power. The isolation ratio is practically power invariant for the first configuration and varies by less than 5 dB over 0-100 W for the second. Each configuration has advantages and disadvantages. In order to decide which one will be used in Advanced LIGO, other aspects, like thermal drift, amount of stray light produced, and space available for proper beam separation, should be considered. Although still to be done, in the three-polarizer configuration we expect to achieve the high performance of the CWP + CWP regarding the optical isolation and of TFP + CWP for beam drift.

For a complete picture, we also examined the beam properties of the laser and described the settings and the experimental methods used.

The isolation and thermal lens measurements were then repeated in vacuum, to account for the additional heating due to the lack of convection.

3 Characterization of the 100 W Laser Beam Properties

3.1 Beam Diameter

3.1.1 Experimental method:

In our measurements we used a CW, custom designed, 100 W IPG Ytterbium fiber laser, model YLR-100-LP. This is a diode-pumped, single-mode, linearly polarized laser, emitting at 1064 nm. To increase the optical path on the available working board, the beam was redirected with a 45° mirror, placed at ~ 60 cm in front of the laser.

We performed point measurements on the beam diameter (measured at $I = I_{max}/e^2$, where I is the beam intensity) with the BeamScan (Photon.Inc XYFIR). At each distance z measured from the laser, the power of the laser was varied by adjusting the set point, waiting to stabilize (5 - 10 minutes), and quickly (< 30 sec), measuring the diameter, before the BS slit heats up and saturates.

3.1.2 Results and Conclusions:

The measured beam diameter along the horizontal and vertical directions, d_x and d_y, is plotted as a function of z-laser in Figure 1. From these diagrams, we can make several observations:

- *The beam narrows as the power increases.* This may reveal some thermal lensing inside laser.

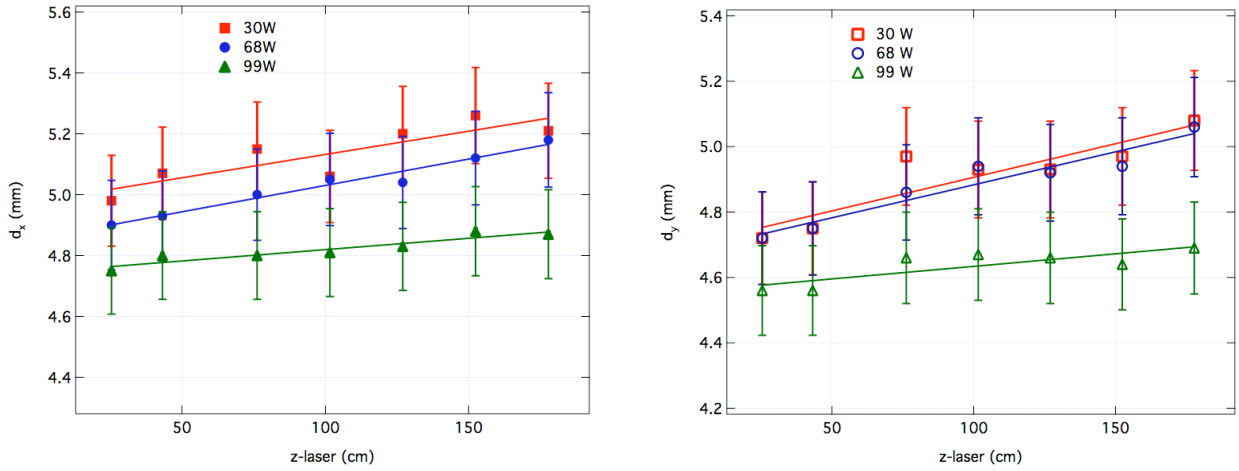

Figure 1: Beam divergence for different optical powers. At 100 W the beam narrows, probably due to thermal effects in the laser's internal optical components, as well as the fiber.

- *The beam presents slight asymmetry,* with an average ellipticity of 1:1.04, as shown in Figure 2.

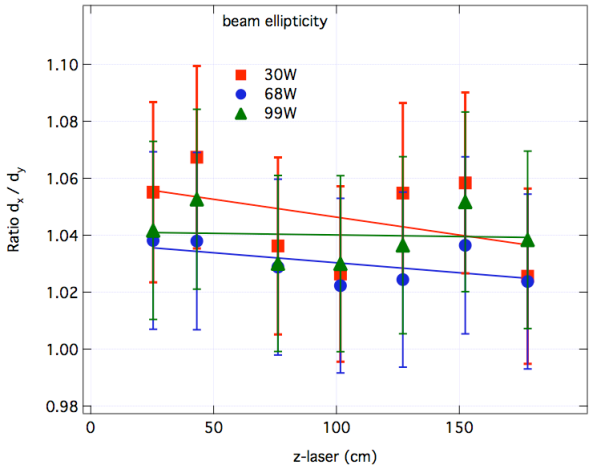

Figure 2: Beam ellipticity at different laser powers.

We can see that the beam maintains this week asymmetry (~ 4%) at all powers, within the error bars (which were selected to account for intensity fluctuations of the laser, the BeamScan detection sensitivity change with the exposing time and uncertainties in z position reading).

3.2 M^2 factor

The M^2 factor is a measure of the beam divergence angle relative to the TEM_{00} mode and practically, it gives the deviation from a perfect Gaussian beam.

3.2.1 Experimental method:

In determining the M^2 factor, we focused the laser to a small spot with a FS lens of focal length f = 40 cm, and we measured the beam diameter using the BeamScan as in Section 3.1, at a number of locations z-laser along the beam propagation direction.

The accuracy in determining the M^2 factor of the laser is limited by the number of points very close to the focus. In order to measure the beam diameter at a number of locations close to the focus, we attenuated the light by replacing the 45^o steering mirror with a fused silica, uncoated plate.

The two diameters of the laser beam were measured at 15 W (real value, measured with the power meter UP55N-300F-H9, and 112 W (read on the laser controller display, which corresponds to ~106 W real value). The standard deviation for x and y beam diameters was ~1.5 %.

3.2.2 Results and Conclusions:

The beam diameter for the two orthogonal directions is plotted in Figure 3 as a function of the propagation distance $z - z_o$, measured with respect to a fixed arbitrary point on the breadboard (the lens).

The M^2 factor for the IPG-YLP laser was determined by fitting the beam diameter with the equation:

$$d(z)=2\bullet\{\omega_0^2+[M^2(z-z_0)/(\pi\omega_0)]^2\}^{1/2}$$

where M^2, the waist w_0, and the z coordinate of the minimum spot z_0, are free fitting parameters. We found 1.17 ± 0.12 for horizontal direction and 1.19 ± 0.11 for vertical direction at 112 W, and 1.03 ± 0.43 for horizontal and 1.17 ± 0.22 for vertical at 15 W.

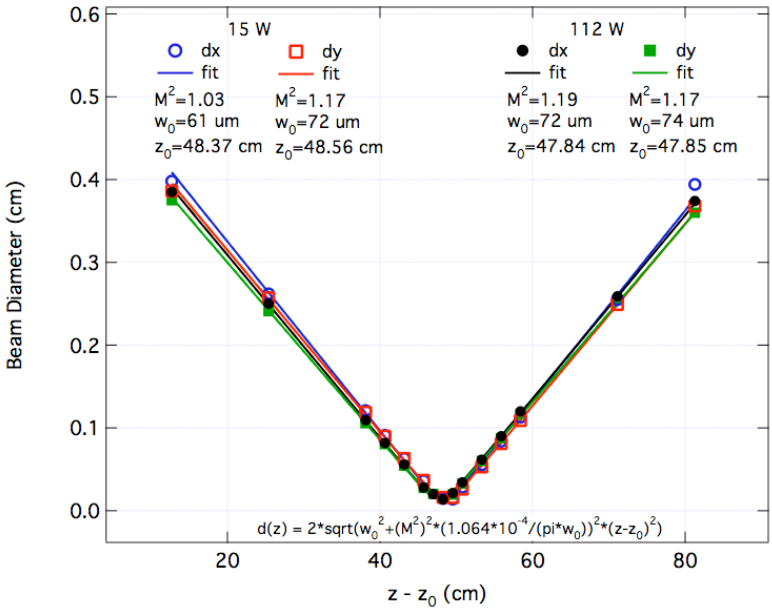

Figure 3: M^2 factor at 15 W and 112 W

A small shift in the beam focus is observed as the power increases (~ 0.7 cm for the change from 20% to 100% operating range), again indicating some thermal lensing of the optics inside the laser, as well as the fiber itself.

4 Characterization of the Faraday Isolator

The Faraday Isolator under tests is equivalent to the one investigated in [1] and explained in detail in [3]. A Faraday Rotator (FR), consisting of two TGG crystals and a quartz rotator (QR), is placed between two polarizers, and a half waveplate, inserted after the FR, rotates the polarization before the second polarizer for maximum isolation.

We investigated the performance of the Faraday isolator in the following two configurations:

- a hybrid configuration consisting of a fused silica thin film polarizer and a calcite wedge polarizer (TFP + CWP), which is optimal for the reflected beam pick-off, and
- a pair of identical calcite wedge polarizers (CWP + CWP), which is ideal for isolation.

However, there are other aspects like thermal drift and scattered light that also play a role in selecting the right polarizers, so we will discuss and compare the performance of the FI in each of these geometries.

4.1 Setup for hybrid configuration TFP + CWP - Figure 4

The original ~ 4.8 mm diameter laser beam was passed through a λ/2 plate in series with a 45° TFP from LZH for power control, redirected with a 45° steering mirror, and send through a second λ/2

plate that optimizes the extinction of polarizers (not required, just convenient for optimum alignment of the TFP). The diameter of the beam was reduced to ~ 3.9 mm with a telescope, consisting of two lenses with focal length f_1 = + 20 cm, f_2 = - 15 cm, separated by ~ 5.5 cm. The beam then passes through the first polarizer of the FI, which is a FS, TFP-1064-PW-2025-UV from CVI, with an extinction ratio of ~ 10^4 at 56^0. The linearly polarized beam passes then through the Faraday Rotator (TGG + QR + TGG in the core of a 1.5 T magnet mounted on a kinematic stage). All three crystals were cleaned in the ultrasound bath for ~ 15 min then wiped with acetone [4]. The most critical piece of optics from the point of view of alignment and also optical quality is the λ/2 plate after the FR, inside the FI, which optimizes (tunes) the isolator.

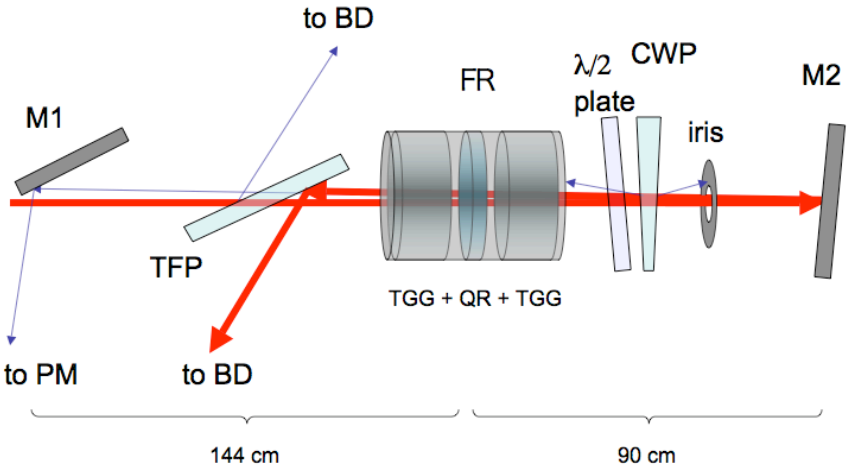

Figure 4: Faraday Isolator: TFP + CWP configuration. The iris blocks the second polarization from hitting the mirror and repropagating back in the FI. It will not be present in the actual design for Advanced LIGO.

We noticed that *optimal isolation was achieved with the plate visibly tilted with respect to the beam (~ 10^o) in the vertical plane.* It seems that this orientation reduces considerably the amount of stray light transmitted back through the isolator, by redirecting the surface reflections in other directions than the beam propagation.

The second polarizer of the isolator was a low absorption 2.5 mm thick calcite wedge polarizer, wedged at 4.3^o from IAP [1]. The extinction ratio of this polarizer is about one order of magnitude higher than the one of the TFP (> 10^5), which makes it very suitable as the polarizer that determines the quality of the beam polarization for the interferometer.

The linearly polarized beam from the second polarizer is reflected back from a 0^o mirror, slightly tilted to separate the back reflection from the incident beam, but keep the beams nearly collinear in the FR. As the two orthogonal polarizations exit the CWP under a very small angle (~1^o), due to the small separation between the CWP and the mirror (about 60 cm), an iris diaphragm is inserted

to block the second polarization from hitting the 0° mirror and repropagating backwards through the isolator.

We collected the backward transmitted light with a 45° pick-off mirror, placed between the telescope and the TFP, very close to the lens (for good separation). The incident and the reflected beams (~ 4mm diameter) were well separated while they also traversed the FR very close to eachother and the center. After careful optimization, the isolation was practically invariant to slight adjustments on the FR. This is a very stable configuration and we could always recover the optimized setting without much difficulty). The distance from the center of the FR to the pick-off mirror was 1.44 m and to the 0° mirror was ~ 90 cm. The CWP was placed about 6" from the end of the FR.

The backward transmitted power was measured with a power meter OPHIR PD300-3W-V1 (also used for all beam powers below 100 mW), and the higher power values with UP55N-300F-H9-DO. We made sure that, at any moment, the beams (incident and backward transmitted) were not clipped and, all the light of interest was collected by the power meters.

4.2 Setup for CWP + CWP configuration - Figure 5

The CVI - TFP was replaced by another calcite wedge and a second 45° mirror was used to direct the suppressed light from propagating back to the laser. The experimental setup was completely realigned due to the angular displacement introduced by the CWP, but all the other optical components are the same as in the TFP + CWP configuration.

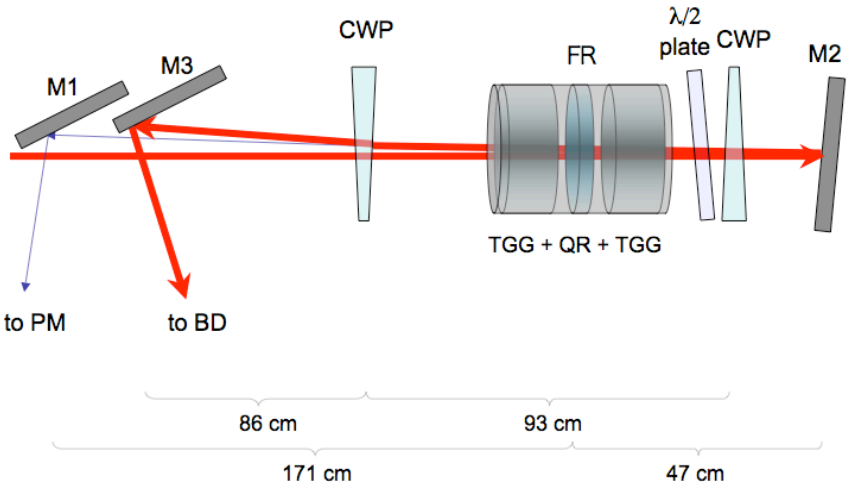

Figure 5: Faraday Isolator: CWP + CWP configuration.

4.3 Optimization and Measurements:

In both setups, the isolator was optimized for minimum back reflection at 103 W incident power (by rotating and tip-tilting the half-wave plate, rotating the TGG and QR crystals in their planes and by changing the separation between first TGG and QR + second TGG, also by adjusting the height (y), and x-z coordinates of the FR).

Once optimized, the FI was not readjusted as the power was lowered from the power control. The laser was given few hours to stabilized before doing systematic measurements. At each power value we measured incident, forward transmitted, backward transmitted and suppressed powers (for the last two we waited 5 - 10 min for the system to thermally stabilize, since the measurements required blocking/unblocking the beam with the power meter, therefore changing the temperature inside the isolator optical components).

At 103 W we observed strong thermal lensing in the FR, the spot diameter decreasing from the low power value of 4 mm to ~ 1.5 mm in ~ 5 m, determining a focal length of 8 m. This is what we expect for the thermally uncompensated FI [1], and can be compensated by inserting a DKDP crystal before or after the FR setup. However, the narrower beam facilitates the FI optimization, by determining a sharper, better-defined spot than at low powers. We constantly checked with a high sensitivity IR card that the back reflected beam hits the pick-off mirror and the detector entirely, and is not cut-off anywhere along the way.

The amount of scattered and stray light in the backward propagating direction was quite large in the CWP + CWP system, mainly because the second polarization from the second wedge could not be separated well within the 25 cm distance to M2. Under a slightly different angle, this beam travels back through the FR and would be collected by M1 as backward transmitted light. However, we were able to separate a significant fraction of this light by placing additional beam stops and irises at large distance from FR (edge stop between CWP and M3, for example), which also blocks a substantial amount light that occurs due to scattering and surface reflections.

4.4 Results and Conclusions:

In the **TFP + CWP** configuration, the maximum power measured for the **backward transmitted** beam was **12.9 mW** at **103 W incident power**, while the **forward transmitted power** was **97 W (94%),** measured in the right polarization, after the iris, in Figure 4.

In the **CWP + CWP** geometry, the **forward transmitted** light (containing both polarizations) was **101 W** at **103 W incident power** (of which 2.8 W in the second polarization), determining that **95%** of the incident light is **transmitted in the first polarization** toward the interferometer, while the highest **backward transmitted** was only **1.3 mW**.

4.4.1 Optical Isolation

The optical isolation determined as the dB ratio between the incident and the backward transmitted light, was **39 dB** for the **TFP + CWP** and **49 dB** in the **CWP + CWP** configuration at **103 W**. The variation across 0-103 W power range is shown in Figure 6.

In both situations the FI was tuned (optimized) at 103 W and not touched thereafter. While the TFP + CWP configuration presents a lower isolation ratio than the CWP + CWP, it is less sensitive to

the overall power change (less than 1 dB change when the power was varied - lowered), is more compact and presents a neater layout and more manageable stray light.

An excellent isolation ratio of 49 dB is obtained at 103 W for CWP + CWP, and this stays above 48 dB for power changes of ~ 30 W (as low as 60 W incident). It decays to 44 dB as the power drops down, mainly due to depolarization changes and rotation of the polarization in the TGG and QR crystals.

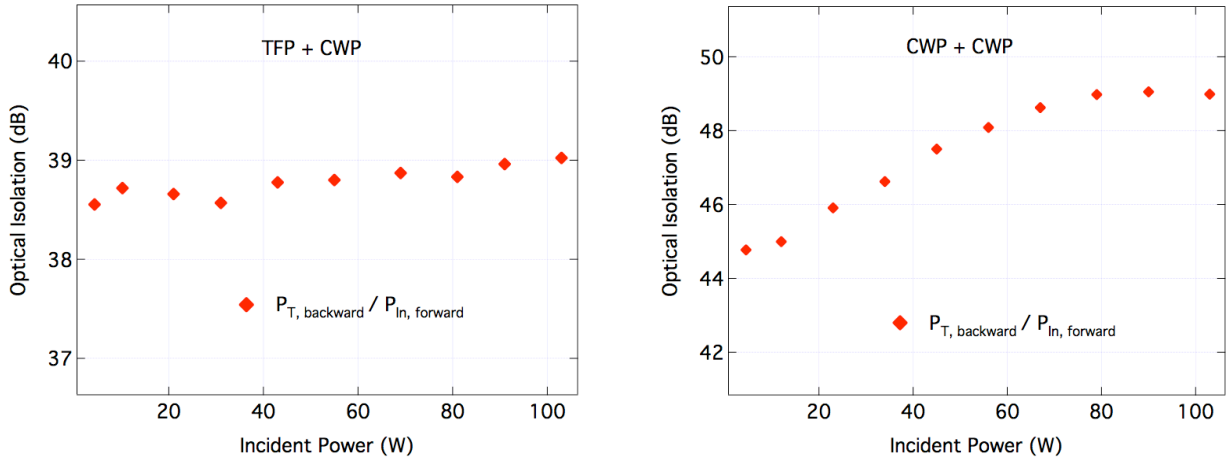

Figure 6: Optical isolation for TFP + CWP (left), and CWP + CWP (right) configurations.

4.4.2 Beam Drift

We measured the beam steering in transmission and back reflection at 103 W incident power, by using a Quadrant Photodetector (QPD). We blocked the beam in front of FI for 45 min, then recorded the drift for 30 minutes. To stay in the detection limits of the QPD, the power was attenuated with AR plate followed by an uncoated FS plate. For the CWP + CWP configuration, an additional NDF was used in front of the QPD when the drift was measured for the transmitted beam.

The noise level is determined by the fluctuations in the laser intensity (much quieter signal was observed at lower powers) together with excessive noise amplification of the QPD. As some optical elements warm up as they are illuminated (0^o mirror that reflects light back into FI as well), we could not separate entirely each thermal effect (of the FI from other optics).

The thermal displacement measured in each configuration for the transmitted and reflected beams is shown in Figure 7, across ~ 2.5 m distance from the FR. A small drift is observed in all four situations, slightly larger in reflection as well as for the two-wedge setup. The largest drift is 80 μrad for CWP + CWP in reflection and the smallest is 20 μrad for TFP + CWP in transmission (average values, the noise level is ± 20 μrad).

These values are consistent with each other and with the value of 40 μrad obtained previously[1] for the double-wedge setup at 30 W power. That the observed drift in reflection is larger than in transmission, can be explained by the fact that the polarizers (calcite wedges in particular) are traversed by the high power beam twice, which is not true in transmission. Also, some "environmental drift" (observed in the 0^o mirror) is not present in transmission. Third, the drift in

the TFP + CWP is smaller that in the CWP + CWP since the thin film polarizer is not wedged, though it introduces no or less thermal shift.

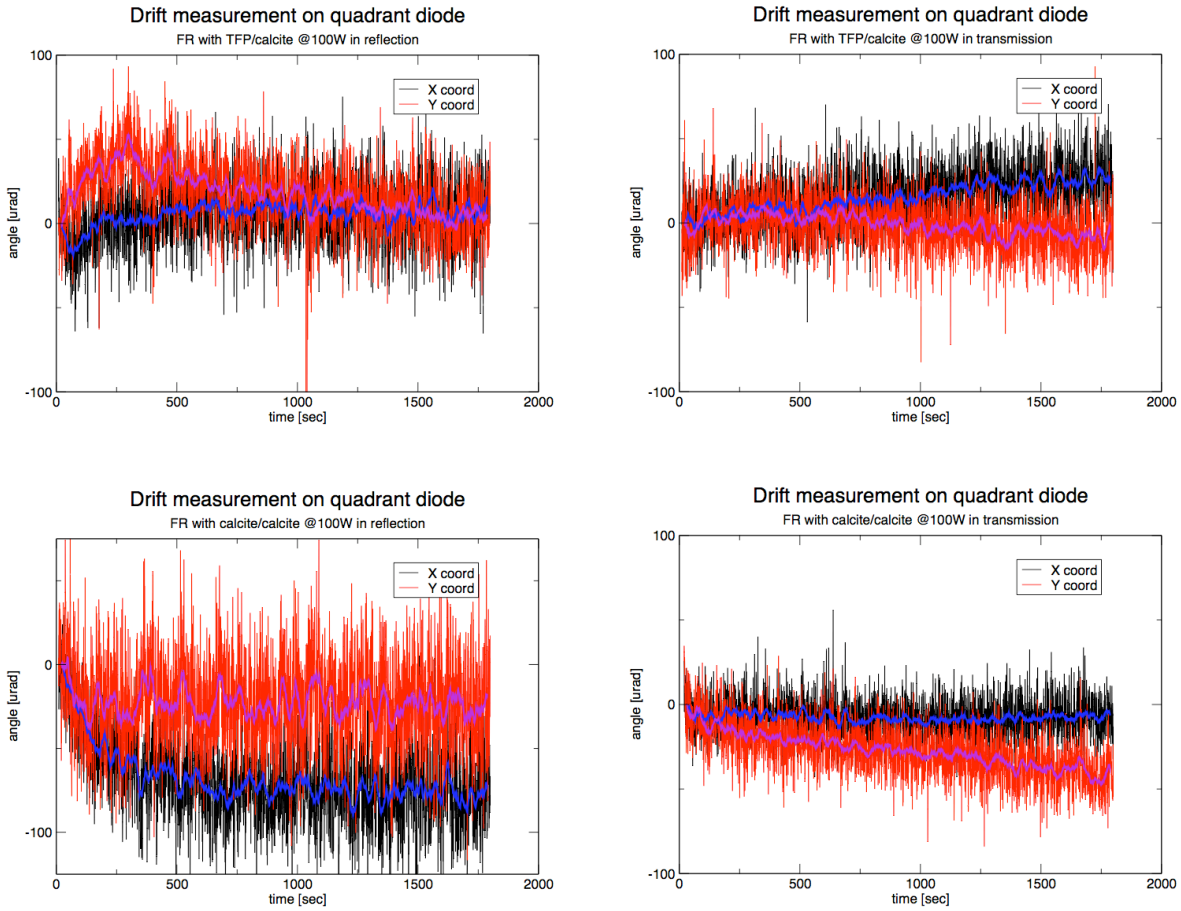

Figure 7: Displacement measurements for the TFP + CWP and CWP + CWP setups in reflection (backward transmission) and (forward) transmission.

4.4.3 Thermal Lens Compensation

Thermal lens compensation was investigated in a previous study[1] in a double calcite polarizer setup, by placing a DKDP crystal after the second polarizer of the isolator. The total thermal lensing observed at 70 W of incident power was -40 m. These measurements were repeated recently at LLO at 30 W laser power and a total thermal lensing of -40 m to -56 m was found. The DKDP crystal slightly overcompensates for the positive thermal lens induced in the TGG crystals. Same measurements were done in vacuum and no significant difference regarding thermal lensing was observed compared to in air measurements.

Other observations were made with the available DKDP:

- The available pieces of DKDP are birefringent, though they are expected to deteriorate the isolation ratio if placed between the two polarizers. New sources of z-cut DKDP are investigated at the present, and new crystals will be tested soon at LLO for ELIGO.

- DKDP is highly hygroscopic, needs desiccant and tight enclosures for storage.

The performances of the FI in air are summarized in Table 1 below.

Table 1: FI performance in TFP + CWP and CWP and CWP configurations at 103 W incident power.

Performance at 103 W		TFP + CWP	CWP + CWP	Comments
Isolation Ratio:		**39 dB**	**49 dB**	Good optical isolation in both setups. **39 dB** is limited by the extinction of the TFP.
Variation in isolation across 0-103 W		*< 1 dB*	*< 5 dB*	*Isolation **worsens** at **lower** powers.*
Back-transmitted:		12.9 mW	1.3 mW	Better suppression for the CWP + CWP setup.
Transmitted: *(in the right polarization)*		94 %	95 %	The FI was optimized for max. isolation (min. back reflection).
Losses:		6 W	5 W	Of which ~ 3 W are lost in the second polarization after the second CWP. Less than 3W (2-3%) is random/stray light.
Thermal Drift: *(±20µrad)*	*Transmission:*	**20 µrad** *(0.2 µrad/W)*	**40 µrad** *(0.4 µrad/W)*	Larger drift for CWP + CWP setup (2 CWPs).
	Reflection:	**40 µrad** *(0.4 µrad/W)*	**80 µrad** *(0.8 µrad/W)*	Drift in reflection is twice as in transmission (CWP double passed).

4.4.4 In-vacuum performance

4.4.4.1 Vacuum compatible magnet housing

A new vacuum compatible housing was designed for the Faraday rotator, and the unit was baked at 80C and passed the outgassing test and showed no degradation of the magnetic field strength after baking. An image of the seven-segment Faraday rotator housing designed for ELIGO is shown in Figure 8 .

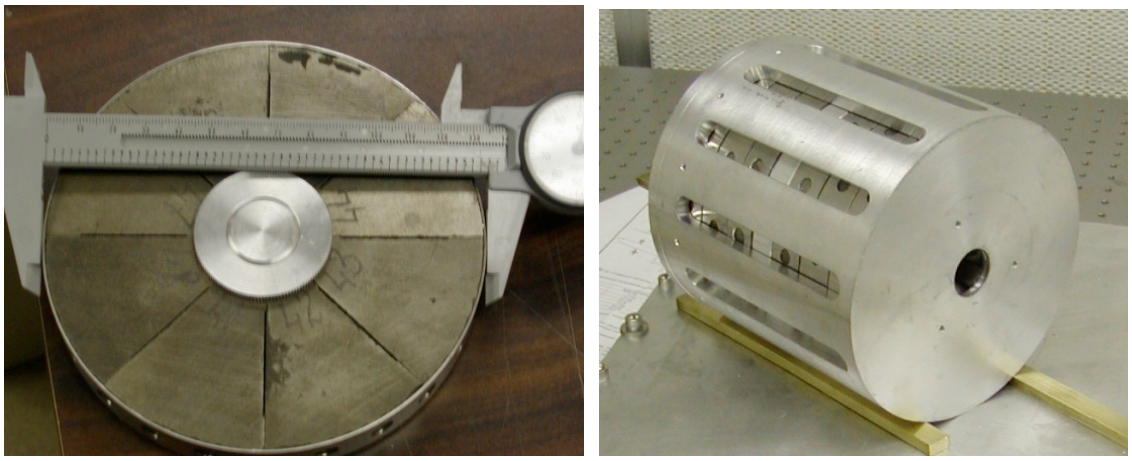

Figure 8. Cross section (one ring out of seven) and housing assembly of the vacuum compatible Faraday rotator.

The magnetic field measured along the magnet axis, for the 5-segment magnet used in our experiments, is shown in Figure 9. The two TGG crystals are placed in about 1T effective magnetic field, symmetrically about the position with the highest field where the quartz crystal is located.

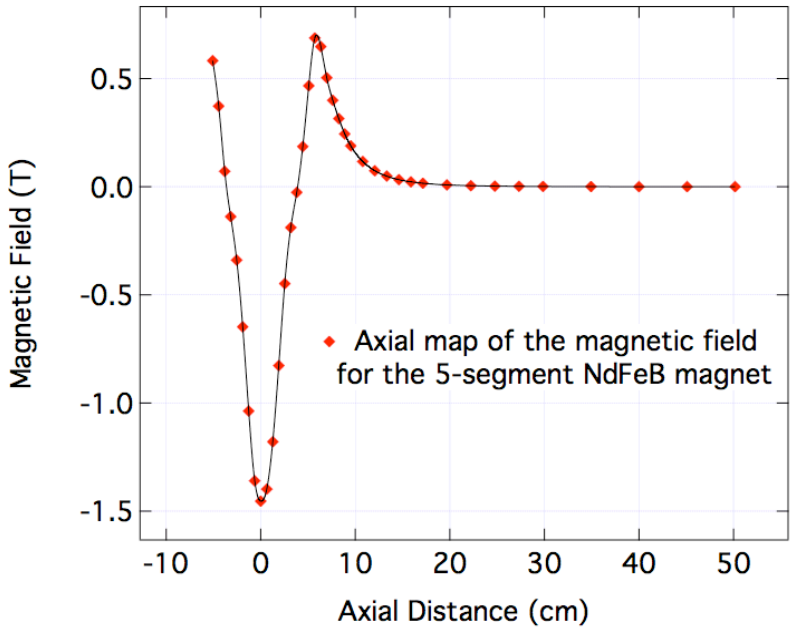

Figure 9. Magnetic field versus distance along the magnet axis

4.4.4.2 Preliminary UHV isolation results:

The Faraday isolator with two calcite polarizeres was tested at 104W, 50W and 30W in vacuum at pressure of 10^{-4} – 10^{-5} Torr. The isolation ratio was optimized at ambient pressure, and was monitored as the pressure was lowered. Preliminary results show strong degradation with increasing the vacuum levels, attributed to the less efficient convection cooling of the absorbing optical elements of the Faraday isolator. The isolation degradation at lower pressure values is shown in Figure 10.

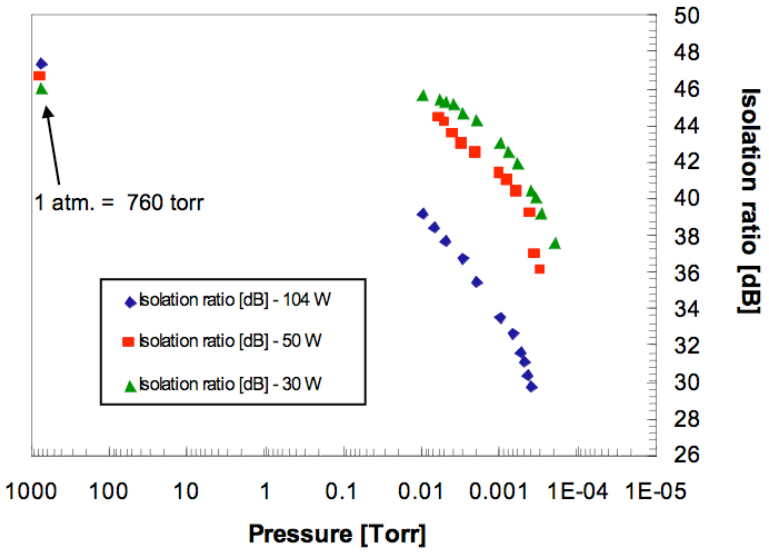

Figure 10. Isolation degradation with pressure, at 104 W, 50 W and 30 W

4.4.4.3 Isolation restoration with in-situ waveplate adjustment

Recently we have inserted a vacuum-compatible motorized rotation stage in the chamber to control the half-wave plate for a better optimization of the isolation. Figure 11 shows that the isolation can be recovered by small adjustments of the half-wave plate in vacuum. For the data shown in the graph on the left (Figure 11a), the system with the 2 calcite polarizers and withouth thermal lens compensation had run for an hour and the waveplate was adjusted for best isolation. Then, the isolation was measured at 10 min intervals during the next 90 minutes, showing a decrease from 40 dB to just below 36 dB. The initial isolation was then recovered by a fractional degree adjustment of the waveplate. There was a small pressure increase, attributed to outgassing of the isolator as the temperature increased.

The experiment was repeated with the DKDP placed in-between the two calcite polarizers and the isolation was recovered again with the motorized half-waveplate (Figure 11b). The isolation was stable after about 12 hrs, even improving slightly due probably to the fact that the waveplate overcompensated at 36 dB, and then the temperature increase produced a more fine adjustment of the polarization rotation that we were able to get with the motor. For Advanced LIGO, a picomotor controlled half waveplate will be inserted to restore the isolation.

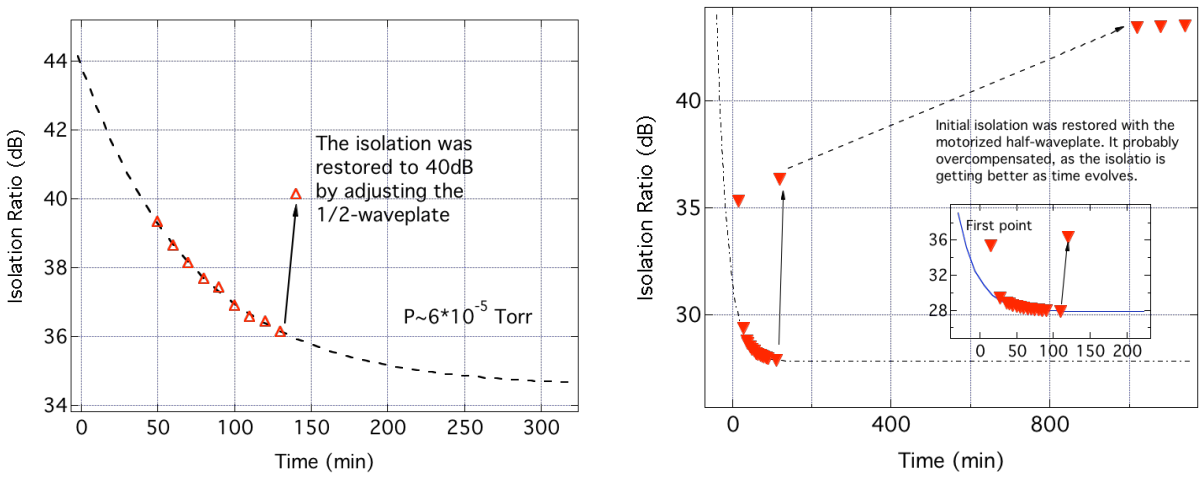

Figure 11. Isolation restoration with the motorized half waveplate: a) FI without thermal compensation; b) FI with DKDP inserted for thermal lens compensation.

4.4.4.4 Thermal modeling to explain the isolation degradation and the restoration

To explain the degradation in the isolation ratio in vacuum, we monitored the light transmitted backward through the isolator (which determines the isolation ratio) as a function of time (represented in Figure 11a), for more than 2 hrs from the moment the laser was turned on. From the measured transmission we estimated the polarization angle θ around 90 deg, using $I_{tr}/I_0 \sim \cos^2(\theta+90)$, I_{tr} and I_0 being the backward transmitted and the incident laser intensities, respectively.

Since the isolation can be completely restored to its initial value by rotating the polarization with the half waveplate, we can assume that this degradation is determined predominantly by the change in the Verdet constant of the TGG crystals with the temperature. From the estimated polarization angle, we determined the temperature change as a function of time using the relation θ(T)=V(T)LB, and known value for the fractional change in the Verdet constant with the temperature from literature. A plot of the temperature T versus time is shown in Figure 12,

Fitting with the equation $T(t) = T_0 + \Delta T \bullet [1-\exp(-t/\tau)]$, we determined a time constant of the system of ~115 min. To determine the time constant of the TGG crystals we should repeat the measurements at much shorter time intervals, of about 5 to 10 seconds, as theoretically we determined a time constant of 0.5 min to 2 min.

The overall temperature change causing the 4 dB degradation in the isolation ratio was found to be less than 1K.

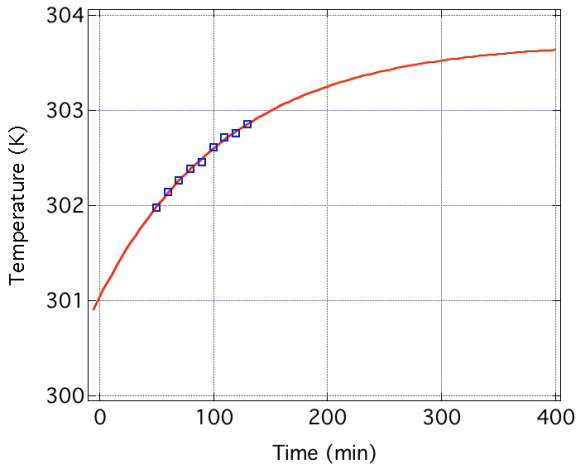

Figure 12. Temperature of the TGG crystals as a function of time and the exponential fit.

From the same isolation ratio measurements we can infer the change in the rotation angle of the polarization with time (Figure 13), and we can see that a less than 0.3 deg rotation is enough to cause the 4 dB deterioration in the isolation ratio observed.

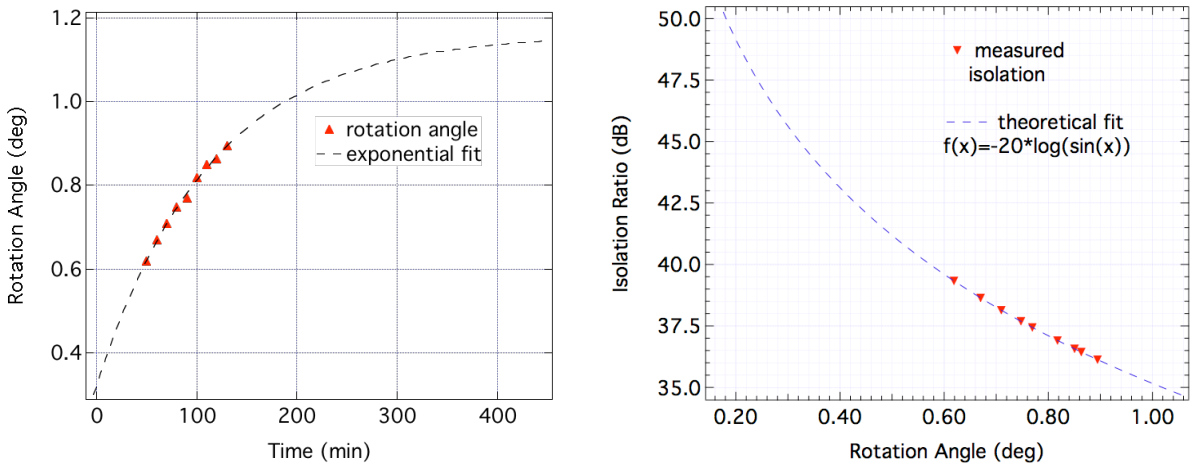

Figure 13. Determination of the rotation of the polarization due to the temperature change of the Verdet constant versus time (left); Dependence of the isolation ratio on the rotation of polarization (right)

4.4.4.5 Design of a TGG holder for more efficient heat transfer by conduction

In addition to restoring the isolation with the waveplate adjustment, we are developing a design that has more effective conduction cooling channels, this way reducing the heat stored in the crystal, though the thermal effects associated with it.

In this design, the TGG crystals are wrapped in a thin layer of indium foil, which is pressed against the walls of the tube by a tapered collet as shown in Figure 14. This way, the TGG crystals inside the magnet are transferring the heat to the indium foil, which then will be conducted trough the aluminum walls of the holder to the exterior of the magnet case.

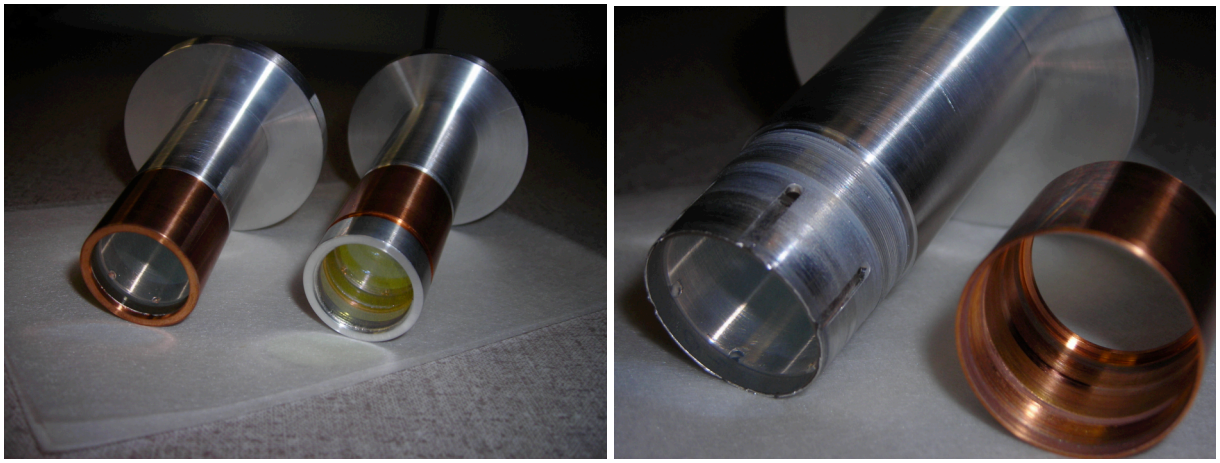

Figure 14. TGG holders designed for more efficient heat transfer by conduction: a) holders for TGG and TGG+quartz; b) open TGG holder to show tapered collet.

5 Conclusions:

The main purpose of this document is to provide an update on Advanced LIGO Faraday Isolator performance using new choice (and different combinations) of polarizers (high extinction ratio thin film polarizer combined with a calcite wedge polarizer), as well as to repeat the study on the isolator based on two calcite wedge polarizers, at a beam diameter close to the value of 4.2 mm set by the MC (we used a 3.9 mm diameter beam, which is within 10% the imposed value).

In these two configurations, we measured the isolation ratio, thermal drift, and thermal lens compensation with a piece of DKDP in the path of the beam. The optical isolation and the beam steering measurements in air did not involve the DKDP in the setup.

The approach in performing the isolation measurements was new: we optimized the isolation ratio at high power, and made no adjustments as the power was systematically lowered. This way, we determined an optical isolation of **39 dB** for the TFP + CWP configuration and **49 dB** for the CWP + CWP setup **at 103 W laser power**.

The better values found in this work compared to the previous results (42 dB at 95W, decreasing as power increases [1]) may be explained by several factors:

- double-size beam diameter causing less thermal depolarization
- higher extinction of the thin film polarizer (> 10^4)
- new measuring approach.

The thermal drift measured at 103 W also showed satisfying results in both setups. For the TFP + CWP combination we measured a drift of 40 μrad (0.4 μrad/W) for the backward transmitted beam, and 20 μrad (0.2 μrad/W) for the forward transmitted light. These values double for the two-wedge setup, where we obtained 80 μrad (0.8 μrad/W) in reflection and 40 μrad (0.4 μrad/W) in transmission (again, with large error bars of about 20 μrad). The double drift increase in this case can be explained by the presence of the additional CWP, which is passed twice for measurements in reflection (backward transmission). The drift measured in the previous experiments [1] was 40 μrad at 30 W incident (1.3 μrad/W) for the two-calcite wedge polarizer setup.

Although the beam drift values are not to be taken as exact for the Faraday Isolator, due to other aspects that contribute to this, like "environmental" drift and intensity noise, they provide an upper limit of the thermal beam steering, when the "rest" of the optics is thermally stabilized (except for the FI and the optics after it in the path of the beam). This accounts more realistically for the overall thermal deviations and only in-vacuum measurements would determine an absolute value of the beam steering in the FI.

For a complete study, we also measured the beam properties of the laser. We found that the beam narrows slightly as power increases (~ 6% from 30 to 99 W), due to probably some thermal lensing in the fiber and in the laser's internal optical components, and that it shows a negligible asymmetry (an average ellipticity rate of 1:1.04). The M^2 factor determined for this laser was 1.19 ± 0.11 for vertical direction and 1.17 ± 0.12 for the horizontal direction at full power (112 W on the laser panel display). These results show that the laser beam has a very good optical quality, and besides the intensity fluctuations at high power, it is found suitable for the purpose of our high power testing of the Faraday Isolator.

We also investigated the performance of the Faraday isolator in vacuum at pressure of $10^{-4} – 10^{-5}$ Torr. We found that the isolation degrades in vacuum due to the lack of convection. To correct for this aspect, we inserted a motorized half waveplate to in-situ restore the isolation, also designed new crystal holders to improve heat conduction toward the exterior of the magnet housing. We studied thermal lensing and found not significant difference compared to the in-air measurements.

---

[1] LIGO-E060267-00-D, "Upgrading the Input Optics for High Power Operation", UF LIGO Group, IAP Group.

[2] Already tested in the CWP + CWP setup, for 2 mm diameter beam[1]. To be redone at 3.9 mm beam diameter with a good piece of DKDP.

[3] E. Khaznov, N. F. Andreev, a. Mal'shakov, O. Palashov, A. K. Poteomkin, A. Sergeev, A. A. Shaykin,V. Zelenogorsky, I. A. Ivanov, R. Amin, G. Mueller, D. B. Tanner, and D. H. Reitze, "Compensation of thermally Induced Modal Distortions in Faraday Isolators" IEEE J. Quantum Electron., 40, 1500-1510 (2004).

[4] Note: all optics were acetone cleaned prior to mounting.